A proton NMR study of the mechanism of the erythrocyte glucose transporter

(membrane/binding sites/sugar transport/sliding-barrier model)

JIN-FENG WANG*, JOSEPH J. FALKE†, AND SUNNEY I. CHAN‡

Arthur Amos Noyes Laboratory of Chemical Physics, California Institute of Technology, Pasadena, CA 91125

ABSTRACT   A generalizable ^{1}H NMR technique is developed and used to monitor β-D-glucose binding to glucose transport sites on erythrocyte membranes. This technique provides resolution of β-D-glucose binding sites on opposite sides of the membrane, thereby enabling study of recruitment of transport sites from one side of the membrane to the other. Cytochalasin B, which competitively and specifically inhibits glucose binding to the inward-facing glucose transport site, recruits all glucose transport sites on both sides of the membrane to the inward-facing conformation. This result strongly supports a one-site model in which a single transport site alternates between distinct inward- and outward-facing conformations. The rate-limiting step in the transport process is translocation of the transport site between the two conformations, since the β-D-glucose binding and dissociation events at both the inward- and outward-facing transport sites are shown to be fast compared to the known turnover rate of the glucose transport cycle. A model is presented for the transport machinery in which the glucose molecule binds in a cleft between channel-forming transmembrane helices, and during the transport event a sliding barrier moves past the transport site, thereby exposing the site to the opposite solution compartment.

The erythrocyte membrane possesses a facilitated transport system specific for D-glucose and certain other monosaccharides. Recent biochemical studies have begun to reveal the molecular nature of this transport system: the human erythrocyte membrane contains approximately 300,000 independent glucose transporters, and the sole constituent of these transport units appears to be a 54-kDa polypeptide, which is heterogeneously glycosylated and has been reconstituted with retention of glucose transport activity (refs. 1 and 2; reviewed in ref. 3; see also ref. 4). A variety of evidence suggests that the monomer associates to form stable dimers and perhaps tetramers in the membrane (3), although the number of monomers constituting an independent transport unit has not yet been determined. The gene for the glucose transporter of human hepatocytes has been sequenced, and a structural comparison of the hepatocyte and erythrocyte proteins indicates that the two proteins are highly homologous or identical (1). Thus, a single glucose transporter species could be a ubiquitous component of cells in higher animals, making the glucose transporter an excellent system in which to study the transport of small molecules across biological membranes.

To develop a molecular picture of the events that occur during glucose transport, it is necessary to (*i*) monitor the behavior of both the inward- and outward-facing transport sites during the transport cycle, (*ii*) determine the chemical and kinetic equations that describe the transport cycle, and (*iii*) investigate the structural change in the transport site that occurs during the transport event. These fundamental questions can now be addressed by NMR techniques. The present paper describes a ^{1}H NMR study of glucose binding to the transport sites on the erythrocyte glucose transporter. This NMR approach reveals that (*i*) transport sites exist on both surfaces of the erythrocyte membrane, (*ii*) these sites can all be recruited to the intracellular surface by cytochalasin B, and (*iii*) the rate-limiting step in the transport cycle is the translocation of bound glucose across the membrane. On the basis of these data, a model describing the binding and transport of glucose is presented.

MATERIALS AND METHODS

Materials. Biochemicals were obtained from Calbiochem–Behring (β-D-glucose and L-glucose) and from Sigma (cytochalasin B). Freshly outdated packed erythrocytes were the kind gift of the Los Angeles Chapter of the American Red Cross.

Preparation of NMR Samples. All procedures were carried out at 0–4°C. Leaky erythrocyte ghosts were prepared exactly as previously described (5). Exchangeable protons were depleted by three cycles of: (*i*) pelleting the membranes (35,000 × *g* for 30 min), (*ii*) resuspension in ^{2}H$_2$O containing 5 mM phosphate, pH 8 (a mixture of NaH$_2$PO$_4$ and Na$_2$HPO$_4$), and (*iii*) extensive swirling on a Vortex mixer to completely resuspend the pellet. The three centrifugation steps cause the bulk of the ghosts to collapse to form crushed ghosts (6). When appropriate, these crushed ghosts were used as noted; in all other cases the crushed ghosts were sonicated as previously described (6). After the addition of cytochalasin B to appropriate samples, the ghost suspensions were transferred to 5-mm NMR tubes and kept on ice until NMR analysis the same day. Except where otherwise indicated, the samples contained approximately 12 mg of total ghost protein per ml, as determined by the modified (7) Lowry *et al.* protein assay (8). Samples compared in the same figure were made from the same batch of membranes and thus contained the same concentration of glucose transporter.

^{1}H NMR. Spectra were obtained on a Bruker WM 500 spectrometer (^{1}H resonance frequency = 500.13 MHz). Spectral parameters were: 23°C, 16,384 data points, 90° pulse, and acquisition time 1.6 sec with a relaxation delay of 3.4 sec, and the unmodified free induction decay was directly Fourier transformed. The number of scans was 16 for standard spectra and 256 for nuclear Overhauser effect (NOE) difference spectra. No settling of ghost membranes occurs on this time scale.

Abbreviations: NOE, nuclear Overhauser effect; β-H$_n$ proton, β-D-glucose proton on carbon *n*.
*Present address: Institute of Biophysics, Academia Sinica, Beijing, People's Republic of China.
†Current address: Department of Biochemistry, University of California, Berkeley, California 94720.
‡To whom correspondence should be addressed.

For measurements of the *intramolecular* NOE between the β-D-glucose protons H_2 and H_4, the residual $^1H^2HO$ signal was suppressed by using the Redfield specific four-pulse sequence (9). The NOE was produced by saturating the β-D-glucose H_4 (β-H_4) proton with 0.002 mW of rf power, while accumulating the NOE difference spectrum. Subsequently the area under the β-H_2 peak was gravimetrically determined and compared to the area obtained for the same peak in a non-NOE spectrum obtained under identical conditions, thereby yielding the NOE in percentage.

Spin lattice relaxation times (T_1) of β-D-glucose protons were measured by using the inversion–recovery pulse sequence. The 180° pulse width was carefully measured for each sample before beginning the pulse sequence. Data were subjected to a nonlinear least-squares analysis to yield the best-fit spin lattice relaxation rates ($R_1 = 1/T_1$). The sample temperature during all NMR experiments was 23.0 ± 0.1°C.

RESULTS

^1H NMR Spectrum of D-Glucose. The D-glucose ^1H NMR spectrum is complicated by the presence of both α and β isomers of D-glucose, which interconvert slowly on tHe NMR time scale so that distinct resonances are observed. All of the protons in the β-D-glucose ^1H NMR spectrum have been assigned by homonuclear decoupling and NOE experiments at 500 MHz (Fig. 1). The spectrum of L-glucose is identical (Fig. 2). Neither the D-glucose nor the L-glucose spectrum contains contributions from hydroxyl protons, which are rapidly exchanged for deuterons in ^2H_2O solutions.

Effect of Macromolecular Binding Sites on the NOE. The NOE changes dramatically when a freely tumbling small molecule in solution binds to a macromolecule (10); thus, the NOE is potentially useful as an assay for macromolecular binding sites. Consider, for example, two protons on a small molecule ligand that lie near each other so that their magnetic dipoles interact. When one proton is irradiated at its NMR
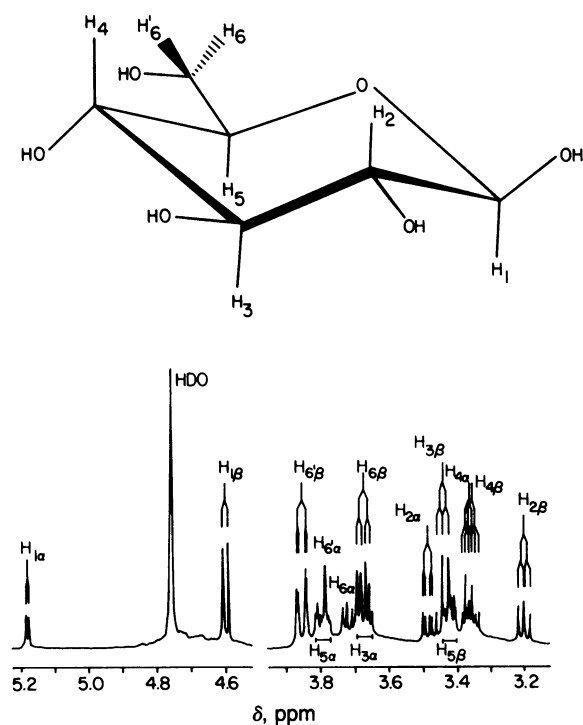
frequency, the NOE alters the intensity of the NMR resonance due to the other proton by the factor $1 + f_I(S)$.

$$f_I(S) = \frac{(\overline{W_2 - W_0})}{(\overline{W_0 + 2W_{II} + W_2})} \frac{\gamma_S}{\gamma_I}, \qquad [1]$$

where I and S are the observation and irradiation nuclei, respectively; W_2, W_{II}, and W_0 are the double, single, and zero quantum transition probabilities for the I, S spin pair (11); and the numerator and denominator are separately averaged over all environments experienced rapidly on the NMR time scale. For a rapidly tumbling molecule in solution, the NOE reduces to $\gamma_S/2\gamma_I = 0.5$ for two protons. For a slowly tumbling

a
D-Glucose

b
D-Glucose
+ ghosts

c
D-Glucose
+ ghosts
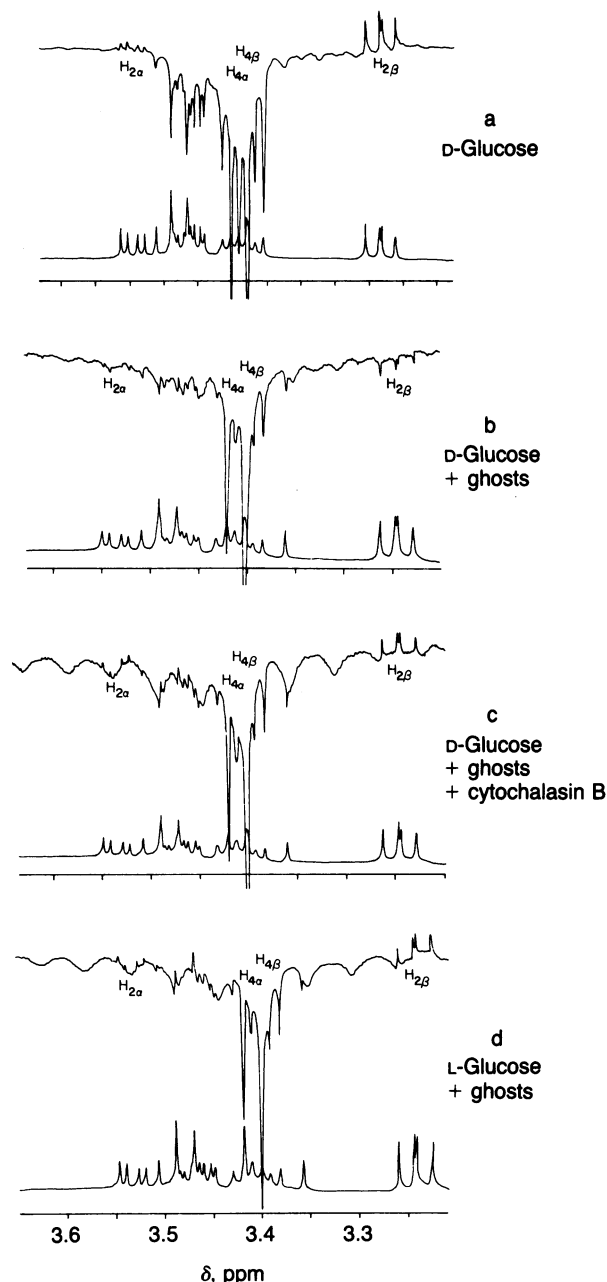+ cytochalasin B

d
L-Glucose
+ ghosts

δ, ppm

FIG. 2. Effect of glucose transport sites on the glucose ^1H NOE difference spectrum. Shown is the ^1H NOE difference spectrum (upper trace) of the β-H_2 proton obtained by irradiation of the β-H_4 proton in the absence (*a*) or presence (*b–d*) of ghost membranes at 23°C ($H_{2β}$ = β-H_2, etc.). Concentrations: 15 mM D-glucose (*a–c*) or 15 mM L-glucose (*d*); 83 μM cytochalasin B (*c*); ghost membranes were 12 mg of total ghost protein per ml (*b–d*).

FIG. 1. D-Glucose ^1H NMR spectrum at 500 MHz. Shown is the structure of the β isomer. In the α isomer, H_1 lies above the ring. The indicated spectral assignments are deduced from homonuclear decoupling and NOE experiments. D-Glucose = 175 mM; 23°C.

Biophysics: Wang *et al.*

Proc. Natl. Acad. Sci. USA 83 (1986) 3279

molecule in a macromolecular binding site, $W_0 >> W_2$ and W_{II} and the NOE reduces to $-\gamma_S/\gamma_I = -1$ for two protons.

To use this NOE binding effect to its full potential, a relationship must be drawn between the observed NOE and the concentration of bound ligand. When the exchange of ligand between solution and a heterogeneous population of binding sites is rapid on the NMR time scale, it can be shown that

$$f_I(S) = P_F \left(\frac{R_F}{R}\right) f_I(S)_F + \sum_j P_{B_j} \left(\frac{R_{B_j}}{R}\right) f_I(S)_{B_j}, \quad [2]$$

where P_X is the fraction of total ligand instantaneously found in environment X; $f_I(S)_X$ is the NOE of I in X, R_X is the spin-lattice relaxation rate of I in X $[= C_1(W_0 + 2W_{II} + W_2)_X]$; R is the exchange-averaged spin-lattice relaxation rate of I in all Xs $[= C_1(\overline{W_0 + 2W_{II} + W_2})]$; and the sum is over all classes of binding sites. Thus, the observed NOE is a weighted average of the NOE in the bound and free environments, weighted according to the fractional spin-lattice relaxation in each environment—i.e., the *product* of the fractional occupancies and the intrinsic spin-lattice relaxation rates of each environment. This expression becomes particularly simple when the concentration of bound ligand is small relative to the total ligand concentration. In this case, $P_F \approx 1$, $P_B << 1$, and $R \approx R_F$ so that Eq. 2 can be written:

$$f_I(S) = f_I(S)_F + \sum_j f_I(S)_{B_j} \left(\frac{R_{B_j}}{R}\right) \frac{[I_{B_j}]}{[I]}, \quad [3]$$

where P_{B_j} has been explicitly given as the fraction of the total I spin population that is instantaneously found in the *j*th class of binding site. Thus, under appropriate conditions the NOE observed for the total population of ligand molecules is linearly related to the concentration of bound ligand ($[L_{B_j}]$ = constant·$[I_{B_j}]$); also, the contributions of different binding sites are additive. These features suggest that the observed NOE can be used as a straightforward assay for macromolecule binding sites, as illustrated by the following observation of glucose binding to sites on erythrocyte membranes.

Selection of Appropriate Nuclei for Observation of NOE. Examination of the D-glucose ^{1}H NMR spectrum (Fig. 1) indicates that the H_2 and H_4 protons of β-D-glucose are an appropriate pair for NOE experiments, since (*i*) the spin-lattice relaxation rate of the β-H$_2$ resonance exhibits the largest fractional increase when binding sites are added (Table 1); (*ii*) the ^{1}H NMR resonances of β-H$_2$ and β-H$_4$ are well-resolved from the [1]H[2]HO resonance and from each other; and (*iii*) the β-H$_2$ and β-H$_4$ protons are <3 Å apart. Thus, the optimal experimental arrangement is to irradiate β-H$_4$ while observing the NOE induced in β-H$_2$. This arrangement immediately satisfies two of the three conditions required for the use of the simplified linear NOE relationship

(Eq. 3): (*i*) for the β-H$_2$ proton, the increase in the spin-lattice relaxation rate caused by glucose transport sites is significant but is still only a small fraction (14%) of the total spin-lattice relaxation rate of that proton (Table 1); and (*ii*) the total concentration of glucose (15 mM) is large compared to the concentration of glucose transport sites (12 μM). The third condition, that glucose exchanges rapidly between the site and solution, also is likely to be satisfied because the binding of glucose to the transport sites is relatively weak ($K_d = $ 5–50 mM, reviewed in ref. 4). Satisfaction of the rapid exchange condition can be confirmed by observation of an effect of the transport sites on the β-H$_2$ NOE.

Effect of Glucose Binding Sites on the NOE. The β-H$_2$ NOE does reveal a population of D-glucose binding sites on ghost membranes: the β-H$_2$ NOE is positive for D-glucose in free solution, but when ghosts are added, the NOE becomes negative (Figs. 2 *a* and *b* and 3). The fact that the entire D-glucose population exhibits this effect indicates that each β-D-glucose molecule in solution rapidly samples glucose binding sites that give a negative NOE. Both the negative sign and the linearity of the observed NOE are completely consistent with the simplified expression for NOE in the presence of rapidly exchanging sites (Eq. 3). An even more rigorous test of this relationship is the magnitude of the observed NOE. The simplified expression (Eq. 3) predicts that binding sites that (*i*) give an intrinsic NOE $= -1$ for bound glucose and (*ii*) contribute 14% to the total spin-lattice relaxation rate of the observation nucleus (Table 1, β-H$_2$ proton) will cause a 14% decrease in the NOE of the observation nucleus (Eq. 3). This predicted value is within experimental error of the measured NOE, 21% (Fig. 4*a*) for cytochalasin B-sensitive glucose binding sites.

Identification of Glucose Transport Sites. The contribution of glucose transport sites to the observed binding site population can be determined by using (*i*) cytochalasin B, which competitively inhibits glucose binding to the transport sites on the erythrocyte glucose transporter (12, 13) and (*ii*) L-glucose, which does not bind to the transport sites (14, 15). The characteristic inversion of the β-H$_2$ NOE (Fig. 2 *a* and *b*) caused by ghost membranes is lost in the presence of saturating cytochalasin B (Figs. 2–4) and is also lost when the β-H$_2$ proton on L-glucose is observed rather than the β-H$_2$ proton on D-glucose (Figs. 2 and 4). In fact, such results indicate that glucose transport sites are the *only* sites that contribute significantly to the inversion. This follows from the observation that inhibition of glucose binding to the transport sites by cytochalasin B (Fig. 4*a*) or by use of
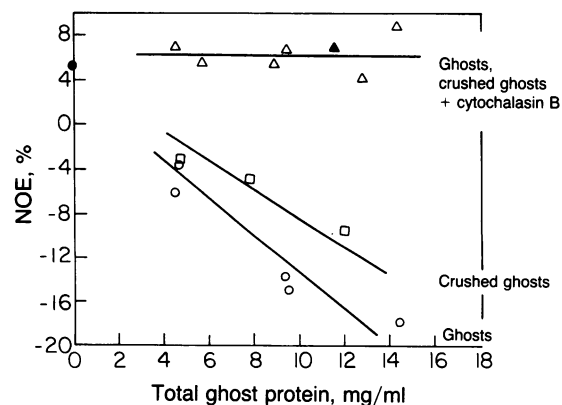
Table 1. Effect of glucose transport sites on the spin-lattice relaxation rates of β-D-glucose protons

Proton	Spin-lattice relaxation rate, sec^{-1}		% of total relaxation due to transport sites
	0 μM cytochalasin B	83 μM cytochalasin B	
H_2	0.21	0.18	14
H_3	0.21	0.19	10
H_4	0.21	0.18	14
H_5	0.24	0.24	0
H_6	0.35	0.37	-5
$H_{6'}$	0.46	0.44	5

The concentration of transport sites was ≈ 10 μM (12 mg of total ghost protein per ml); D-glucose was 15 mM. Replicate experiments confirmed the given relaxation rates to within $\pm 5\%$.

FIG. 3. Dependence of the β-D-glucose H_2 NOE on the concentration of binding sites. D-Glucose was 15 mM: ●, without ghost membranes; ○, with ghost membranes; □, with crushed ghost membranes; △, with ghost membranes and 83 μM cytochalasin B; ▲, with crushed ghost membranes and 83 μM cytochalasin B. Measurements were at 23°C.
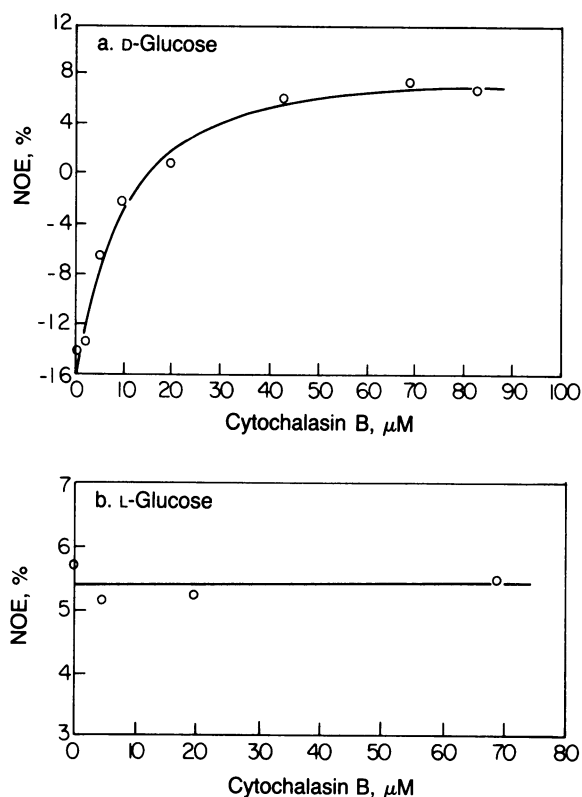
FIG. 4.   Effect of cytochalasin B on the glucose β-H_2 NOE. The data are for 15 mM D-glucose (*a*) or L-glucose (*b*) in the presence of ghost membranes at 12 mg of total ghost protein per ml; 23°C.

L-glucose instead of D-glucose (Fig. 4*b*) restores the β-H_2 NOE to essentially the same value observed in the absence of membranes (+5%, Fig. 3). Thus, the NOE experiment enables sensitive and specific observation of glucose binding to transport sites on the erythrocyte membrane.

Sidedness of the Transport Sites. The NOE assay for glucose binding enables resolution of binding sites on opposite sides of the membrane so that rigorous tests of models for the transport cycle are possible. The sidedness resolution stems from the requirement that the NOE inversion is observed for a D-glucose population only when this population rapidly samples both the binding sites and solution. It has previously been shown by ^{35}Cl NMR that binding sites in the internal compartment of ghost membranes are sampled more slowly by the bulk solution chloride after the membranes are crushed by centrifugation to form hemispherical structures that have negligible internal volume (6). As a result the contribution of inward-facing glucose transport sites to the NOE inversion can be determined by quantitating the fraction of the inversion that is lost when ghosts are crushed. The results indicate that 25% of the observed NOE inversion stems from inward-facing transport sites and that both inward- and outward-facing transport sites are completely inhibited by cytochalasin B (Fig. 3). At first glance this result is surprising because each glucose transport unit is known to possess only one cytochalasin B binding site, which competitively and specifically inhibits glucose binding to the inward-facing transport site (16, 17). The observed simultaneous inhibition of both inward- and outward-facing transport sites strongly disfavors models in which each transport unit has two transport sites simultaneously exposed to opposite sides of the membrane, since such models predict that cytochalasin B should inhibit only the inward-facing site. Instead the results strongly support a model in which the transport unit has a single transport site that is alternately exposed to opposite sides of the membrane, such that cytochalasin B can

inhibit all of the sites by recruiting them to the inhibited inward-facing conformation.

Kinetics of Glucose Binding and Dissociation at the Transport Site. The macroscopic process of glucose transport can be dissected into at least three microscopic events: (*i*) binding of substrate, (*ii*) translocation across the membrane, and (*iii*) dissociation. An adequate picture of the transport process must include knowledge of the rate-limiting microscopic event. The present NOE inversion results indicate that glucose in solution rapidly samples transport sites on both sides of the membrane during the ^{1}H NMR time scale; this information can be used to calculate lower limits for the glucose on- and off-rates at the transport site. The NMR time scale in this experiment is ≈ 1 sec, and during this time each glucose molecule visits many transport sites; therefore, there are $>>1$ binding events per glucose molecule per sec. However, there are 10^3 times more glucose molecules than glucose transport units [glucose = 15 mM, transport unit = 12 μM, assuming 300,000 transport units per ghost (18)], so that the rates of binding and dissociation events at the transport site are $>>10^3$ events per site per sec. In contrast, the known turnover rates are slower both for the net transport of glucose (300 molecules per site per sec) and for the one-for-one exchange of two glucose molecules [2 × 10^3 pairs of molecules per site per sec (reviewed in ref. 2)]. Thus, the rate-limiting step in glucose transport is the translocation of bound glucose across the membrane, rather than glucose binding or dissociation at the transport site.

DISCUSSION

An acceptable model for the molecular mechanism of the erythrocyte glucose transporter must explain a number of experimental results. The present study strongly supports the previous suggestion that the transport unit possesses a single transport site that is alternately exposed to opposite sides of the membrane (19), such that cytochalasin B binding recruits all sites on both sides of the membrane to the inhibited inward-facing conformation. Such a model accounts for both types of transport catalyzed by this system. In net transport, the unique transport site carries D-glucose in one direction but returns empty, thereby yielding the net transport of a single D-glucose molecule across the membrane. In equilibrium exchange, the transport site carries D-glucose in both directions, thereby producing the one-for-one exchange of two D-glucose molecules across the membrane. The rate-limiting step for both types of transport is the translocation of the transport site across the membrane, since the present study shows that D-glucose binding and dissociation at the transport sites on both surfaces of the membrane are rapid ($>>10^3$ events per site per sec) compared to the turnover rates of net transport (3 × 10^2 events per site per sec) and equilibrium exchange (2 × 10^3 events per site per sec, reviewed in ref. 2). Finally, the D-glucose molecule appears to retain a fixed orientation during the translocation process, since D-glucose derivatives possessing a bulky substituent at C-6 bind more tightly to the outward-facing transport site, while the converse is true for bulky substituents at C-1 (20). The present results are completely consistent with this model for the glucose binding interaction: the spin-lattice relaxation rates of the protons on C-2, 3, and 4 are more enhanced by the presence of transport sites than are the rates of the protons on C-5 and 6 (Table 1), suggesting that in the bound state the former protons interact with spin diffusion pathways in the transport site, while the latter protons are exposed to the solution bordering the transport site.

The final advance in understanding the glucose transport cycle will be the development of a molecular picture that accurately describes the translocation of the transport site across the membrane. It is now possible to propose a
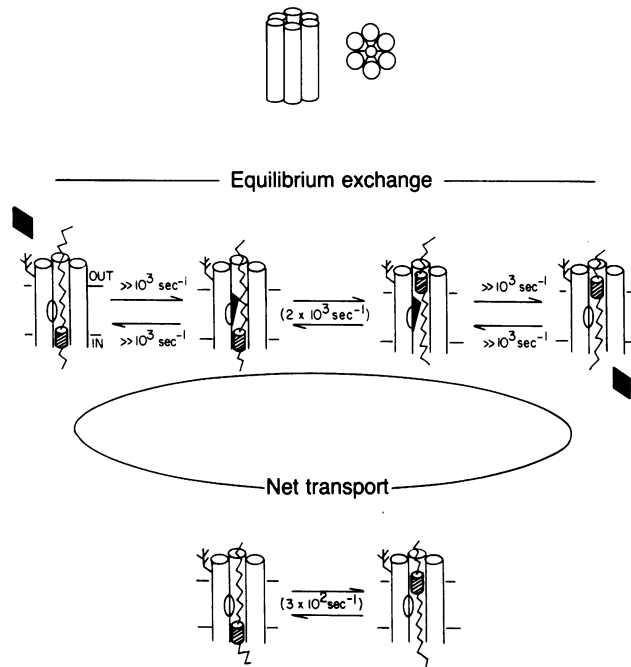
FIG. 5. Equilibrium exchange and net transport of β-D-glucose: Kinetics and a model. Shown are the equilibrium exchange and net transport cycles for an erythrocyte glucose transporter possessing a single transport site that is alternately exposed to opposite sides of the membrane. The indicated rates are events per transport site per sec measured at 23°C in the present work, or elsewhere (rates in parentheses, reviewed in ref. 1). Also shown, at the top, is a schematic representation of a model for the structure of a glucose transporter monomer. The channel-forming α-helices surround a sliding barrier, which is a helical plug connected to segments of random coil. The sliding of the barrier past the occupied (upper path) or empty (lower path) transport site is the rate-limiting step in both equilibrium exchange (upper path) and net transport (circular path).

molecular model that is consistent with a variety of experimental results. Consider, for example, the sliding-barrier model (Fig. 5). This model proposes a transport unit containing a channel surrounded by six or more transmembrane α-helices: sufficient transmembrane α-helices appear to exist for such a model, since the gene sequence of the hepatocyte glucose transporter suggests the presence of 12 membrane-spanning α-helices (1). Inside the channel is a sliding helical barrier that prevents free diffusion through the channel. The D-glucose molecule binds to a transport site in a cleft between two of the channel-forming helices so that C-2, 3, and 4 lie within the cleft, while C-1, 5, and 6 lie outside the cleft. During the translocation event the sliding barrier migrates from one side of the membrane, past the transport site, to the other side of the membrane. This sliding mechanism can explain the observation that equilibrium exchange is faster than net transport, since binding of glucose between channel helices could cause expansion of the channel, thereby allow-

ing the barrier to slide more easily when the transport site is occupied than when empty. However, the sliding of the barrier is always slower than D-glucose binding or dissociation, such that barrier sliding is the rate-limiting step in both types of transport. The sliding-barrier model presented here shares important features with a sliding hydrophobic barrier model that has been proposed for the equilibrium exchange of chloride by band 3, the anion transport protein of erythrocyte membranes (21). Further work will be necessary to ascertain whether sliding barriers or other types of molecular machinery are universal components of transport proteins in biological membranes.

1. Mueckler, M., Caruso, C., Baldwin, S. A., Panico, M., Blench, I., Morris, H. R., Allard, W. J., Lienhard, G. E. & Lodish, H. F. (1985) *Science* **229**, 941–945.
2. Kashara, M. & Hinkle, P. C. (1976) *Proc. Natl. Acad. Sci. USA* **73**, 396–400.
3. Wheeler, T. J. & Hinkle, P. C. (1985) *Annu. Rev. Physiol.* **47**, 503–517.
4. Shelton, R. L. & Langdon, R. G. (1983) *Biochim. Biophys. Acta* **733**, 25–33.
5. Falke, J. J., Pace, R. J. & Chan, S. I. (1984) *J. Biol. Chem.* **259**, 6472–6480.
6. Falke, J. J., Pace, R. J. & Chan, S. I. (1984) *J. Biol. Chem.* **259**, 6481–6491.
7. Markwell, M. A., Haas, S. M., Bieber, L. L. & Tolbert, N. E. (1978) *Anal. Biochem.* **87**, 206–210.
8. Lowry, O. H., Rosebrough, N. J., Farr, A. L. & Randall, R. J. (1951) *J. Biol. Chem.* **193**, 265–275.
9. Redfield, A. G. (1978) *Methods Enzymol.* **49**, 253–270.
10. Clore, C. M. & Gronenborn, A. M. (1982) *J. Magn. Res.* **48**, 402–417.
11. Schuh, J. R. & Chan, S. I. (1982) *Methods Exp. Phys.* **20**, 1–52.
12. Zoccoli, M. A., Baldwin, S. A. & Lienhard, G. E. (1978) *J. Biol. Chem.* **253**, 6923–6930.
13. Sogin, D. C. & Hinkle, P. C. (1978) *J. Supramol. Struct.* **8**, 447–451.
14. Lacho, L., Wittcke, B. & Kromphardt, H. (1972) *Eur. J. Biochem.* **25**, 447–454.
15. Lin, S., Lin, D. C. & Flanagan, M. D. (1978) *Proc. Natl. Acad. Sci. USA* **75**, 329–333.
16. Deves, R. & Krupka, R. M. (1980) *J. Biol. Chem.* **255**, 11870–11874.
17. Basketter, D. A. & Widdas, W. F. (1978) *J. Physiol.* **278**, 389–401.
18. Jones, M. N. & Nickson, J. K. (1980) *FEBS Lett.* **115**, 1–8.
19. Baldwin, S. A. & Lienhard, G. E. (1981) *Trends Biochem. Sci.* **6**, 209–210.
20. Barnett, J. E. G., Holman, G. D., Chalkley, R. A. & Munday, K. A. (1975) *Biochem. J.* **145**, 417–429.
21. Falke, J. J. (1985) Dissertation (California Institute of Technology, Pasadena, CA).